Journal of Petroleum Science and Engineering 78 (2011) 321–327

Contents lists available at ScienceDirect

Journal of Petroleum Science and Engineering

journal homepage: www.elsevier.com/locate/petrol

Applicability of the 'cubic law' for non-Darcian fracture flow

P.G. Ranjith *, D.R. Viete

Department of Civil Engineering, Monash University, Melbourne, Australia

ARTICLE INFO

Article history:
Received 14 September 2010
Accepted 27 July 2011
Available online 7 August 2011

Keywords:
fracture flow
cubic law
non-Darcian
Forcheimer number

ABSTRACT

The influence of inertial effects on the flow of fluids through fractured media is a topic of interest for a number of engineering applications, particularly within the energy sector (e.g. production from gas and oil reservoirs, heat extraction from enhanced geothermal systems, coal-bed methane production). The 'cubic law' can provide a simple relationship between the hydraulic aperture of a fracture and its permeability, for Darcian flow of a given fluid. At significant flow velocities, fracture flow becomes non-Darcian, the velocity–permeability relationship becomes non-linear and the cubic law becomes invalid. However, for transitional flow, which retains a component of linearity, the cubic law may still be applicable for initial determination of superficial velocities from flow rate data. Here, the results of fluid flow experiments carried out for air flow through a fractured granite sample under various pressures of confinement are presented. Analysis of the flow data using the cubic law produced valid results for non-Darcian flow cases where inertial effects were modest. The cubic law appears to be applicable for flow cases that, following analysis using the cubic law, return a Forcheimer number <1.30.

1. Introduction

Numerous aspects of society are dependent on systems involving fluid flow through fractured media. The stability of construction-, mining- or otherwise-induced modifications to the natural landscape is highly dependent on the presence of fluids in the soil and/or rock mass, often hosted in joints, fractures or other defects. Flow through fractured media controls production from gas and oil reservoirs in the petroleum industry. Emerging industries within the sustainable energy sector (e.g. enhanced geothermal energy, coal bed methane, Carbon dioxide (CO_2) sequestration in geological media) require intimate knowledge of fluid flow through fractured media. With a view toward socially and environmentally responsible development and exploitation of our natural environment, an increased understanding of fluid flow through fractured media is imperative.

Kohl et al. (1997) investigated non-Darcian flow behaviour in fractured rock using the results of field flow tests on an enhanced geothermal energy test site. Their manuscript ended with the following statement: "The importance of a general investigation of nonlaminar hydraulic flow patterns in fractured rock should lead to new efforts in designing laboratory… experiments with real fractures. The necessary flow laws for the transition between Darcy and nonlaminar flow can thereby be extended…" (Kohl et al., 1997, p. 417). Here we present a study into the gap in knowledge that Kohl et al. (1997) recognised.

The study addresses issues arising from the influence of a phenomenon known as 'the inertial effect' on the relatively poorly understood mechanisms of fracture flow. Experimental results from air flow tests conducted on a fractured granite specimen under triaxial test conditions are reported. The 'cubic law' expression, discussed by Witherspoon et al. (1980) for a Darcian flow in a parallel-plate model, is used to extract flow velocities for the experimental work from the flow rate data. The applicability of the cubic law to scenarios for which fracture flow has become non-Darcian is explored by interpretation of the experimental data acquired with its application. This laboratory-based study contributes to existing literature (numerical modelling studies) concerning the applicability of flow laws developed for laminar flow models to porous (Mazaheri et al., 2005) and fracture flow (Nazridoust et al., 2006) scenarios that incorporate inertial effects.

1.1. The inertial effect

The concept of permeability is integral to the study of fluid (gas and/or liquid) flow in fractured media. According to Darcy's Law, permeability is constant and is dependent only on the properties of the porous media (e.g. porosity and connectivity). However, it is now understood that flow conditions can also influence the permeability of a porous flow system (see Holditch and Morse, 1976; Rose, 1945; Tek et al., 1962).

Forchheimer (1901) recognised that, as flow velocity in porous media increases, an additional influence on the flow is introduced. He related this behaviour to increasing frictional losses with increasing turbulence in the flow regime. This phenomenon is often referred to as the inertial effect. The inertial effect (represented by Forchheimer's equation) for flow in porous media becomes more significant with an increase in permeability, flow velocity and/or flow pressure conditions (Ruth and Ma, 1992; Whitaker, 1996).

* Corresponding author.
E-mail address: ranjith.pg@monash.edu (P.G. Ranjith).

0920-4105/$ – see front matter © 2011 Elsevier B.V. All rights reserved.
doi:10.1016/j.petrol.2011.07.015

The Reynolds number for flow has been widely used to quantify the degree of influence expected for inertial effects in a flow system (e.g. Rose, 1945; Tek et al., 1962). Bear (1972) suggest flow becomes non-laminar (non-Darcian) for Reynolds numbers (Re) greater than one, but that a transitional flow regime (that may display aspects of Darcian behaviour) dominates for Re = 1 to 10. His recommendations are consistent with those of Zimmerman et al. (2004), who observed complete inertial effects for Re>20, but recognised the influence of 'weak' inertial forces in producing non-linearity for fracture flow regimes with Re = 1 to 10. Hassanizadeh and Gray (1987) proposed that non-linearity in flow through porous media becomes increasingly significant with increasing Re for porous flow regimes with Re>10. Zimmerman and Bodvarsson (1996) showed that roughness in fracture systems leads to increased tortuosity in flow and thus non-Darcian behaviours – relating to increased interaction between the solid and flowing fluid – under flow conditions where they may otherwise not be expected, thus accounting for inertial effects at low values of Re.

2. Background theory

2.1. Darcy's Law

Darcy (1856) published the results of simple experiments carried out to investigate the flow of water through sand. He found that the discharge rate of water through porous sands was proportional to the pressure drop across the flow path, with a constant of proportionality (a resistance to flow) that was specific to the porous medium. Neglecting gravity effects on flow, Darcy's Law for one dimensional flow of an incompressible fluid through porous media can be expressed as:

$$\frac{dP}{dx} = \frac{Q}{A}\frac{\mu}{k}; \tag{1}$$

where Q is the volumetric flow rate; A is the flow area; k is the permeability of the porous medium; μ is the dynamic viscosity of the fluid, and dP is the pressure drop over distance dx in the direction of flow. The superficial fluid velocity (v_s) can be calculated by dividing the outlet volumetric flow rate (Q) by the total free-flow area (A), giving an alternative expression for Darcy's Law:

$$\frac{dP}{dx} = \frac{\mu}{k}v_s. \tag{2}$$

For a compressible fluid (assumed an ideal gas) experiencing isothermal flow, Darcy's Law Eq. (2) can be integrated to produce a quantitative expression that can be used to calculate permeability from experimental results. Innocentini et al. (1999a) gives such an expression:

$$\frac{P_i^2 - P_o^2}{2PL} = \frac{\mu}{k}v_s, \tag{3}$$

where P_i is the inlet pressure; P_o is the outlet pressure; P is the pressure at which μ and (v_s) are measured or calculated ($P = P_c$ for fracture flow in a triaxial experiment carried out at confining pressure P_c), and L is the flow distance across the experimental sample. The form of Eq. (3) is such that, knowing μ, k can be obtained from the slope of the linear curve that that passes through the origin and joins experimental data points plotted in $\frac{P_i^2 - P_o^2}{2PL}$ v. v_s space.

The mean pressure (P_m) for an experiment setup can be calculated from the average of P_i and P_o:

$$P_m = \frac{P_i + P_o}{2}. \tag{4}$$

2.1.1. For fracture flow

Fracture flow is often idealised as flow through a volume bounded by two parallel plates. For such flow geometry, the total free-flow area is calculated by $A = ew$, where e is hydraulic aperture and w is the width of the fracture joint. Witherspoon et al. (1980) provided an expression for fluid permeability in Darcian flow of an incompressible fluid through a fracture idealised as a parallel plate model:

$$k = \frac{e^2\rho g}{12}; \tag{5}$$

where ρ is the fluid density, and g is acceleration due to gravity.

After substitution, Darcy's Law for flow of an incompressible fluid through a fracture becomes:

$$\frac{dP}{dx} = Q\frac{12\mu}{e^3 w\rho g}, \tag{6}$$

and

$$e = \left(\frac{12Q\mu}{w\rho g}\frac{dx}{dP}\right)^{\frac{1}{3}}. \tag{7}$$

For Darcian flow of a compressible fluid within a fracture, Eq. (6) becomes:

$$\frac{P_i^2 - P_o^2}{2PL} = Q\frac{12\mu}{e^3 w\rho_c g}, \tag{8}$$

and

$$e = \left(\frac{12Q\mu}{w\rho_c g}\frac{2PL}{P_i^2 - P_o^2}\right)^{\frac{1}{3}}. \tag{9}$$

For isothermal flow of an ideal gas, gas density is directly proportional to gas pressure and volumetric gas flow is inversely proportional to gas pressure. Thus, ρ and Q for a gas at pressure P can be determined from the known density (ρ_o) and measured flow rate (Q_o) at (P_o), by $\rho = \frac{\rho_o P}{P_o}$ and $Q = \frac{Q_o P_o}{P}$, respectively. Eq. (8) is commonly known as the cubic law.

2.2. Non-Darcian flow

As fluid velocity increases and flow within the porous or fractured media becomes non-Darcian, dependence between the pressure gradient term and the velocity term of Darcy's Law becomes non-linear (Forchheimer, 1901) — i.e. permeability becomes dependent on flow velocity. This dependency is related to the influence of inertial effects.

2.2.1. The Reynolds number in flow through fractured media

The Reynolds number, proposed by Reynolds (1883), provides an indication of flow regime (laminar v. non-laminar) based on the geometry of the flowing system and the properties of the fluid. It can be expressed as:

$$\mathrm{Re} = \frac{\rho Q l}{\mu A}; \tag{10}$$

where l is the characteristic dimension of the flow system. For flow between two parallel plates, with $w \gg e$ (as in an idealised case of fracture flow) $l = e$ (Fox et al., 2004), and thus:

$$\mathrm{Re} = \frac{\rho Q}{\mu w}. \tag{11}$$

2.2.2. The Forchheimer equation for inertial effects

Forchheimer (1901) introduced an empirical constant to account for the non-linearity of Darcy's Law at high flow rates, producing a modified version of Eq. (2) of the form:

$$\frac{dP}{dx} = \frac{\mu}{k} v_s + \rho\beta v_s^2; \tag{12}$$

where β is an empirical constant that accounts for the dependency of k on v_s. Eq. (12) can be written as:

$$\frac{dP}{dx} = \frac{\mu}{k_0} v_s(1 + Fo); \tag{13}$$

where k_0 is the permeability limit for the system as $v_s \rightarrow 0$, and Fo is the Forchheimer Number, given by $Fo = \frac{\rho k_0 \beta v_s}{\mu}$. Eq. (13) shows that, as $Fo \rightarrow 0$, inertial effects become negligible and Forchheimer's equation reduces to Darcy's Law.

For a compressible fluid (assumed an ideal gas) experiencing isothermal flow, Eq. (12) can be integrated to produce a quantitative expression that can be used to calculate permeability from experimental results. Innocentini et al. (1999b) gives such an expression:

$$\frac{P_i^2 - P_o^2}{2PL} = \frac{\mu}{k_1} v_s + \frac{\rho}{k_2} v_s^2; \tag{14}$$

where k_1 can be thought of as the Darcian (viscous) permeability, and k_2 as the non-Darcian (inertial) permeability. Both k_1 and k_2 can be considered as properties only of the porous medium. The values of μ, ρ and v_s used in Eq. (14) should be those measured at pressure P. Considering the Forchheimer Number, Eq. (14) can be rewritten as:

$$\frac{P_i^2 - P_o^2}{2PL} = \frac{\mu}{k_1} v_s(1 + Fo); \tag{15}$$

where $Fo = \frac{\rho k_1 v_s}{\mu k_2}$.

The form of Eq. (14) is such that the k_1 and k_2 can be obtained from the coefficients of the quadratic function that best fits the experimental data points, plotted in $\frac{P_i^2 - P_o^2}{2PL}$ v. v_s space.

3. Experimental procedure

3.1. Sample information

All laboratory work was carried out using a cylindrical granite specimen 104 mm in length and 54 mm in diameter. The cylindrical sample had a single, natural, sub-vertical fracture running the length of the core (Fig. 1). The matrix permeability for the granite used in the laboratory program is low (approximately 10^{-19} m^2, Ranjith et al., 2006, p. 219) and can be assumed to be negligible in comparison with the fracture permeability. Thus, flow in the experiments can be considered to have occurred solely by fracture flow.

Qualitatively, the joint surfaces appeared to join well together, the joint was relatively smooth, and showed no evidence of prior shear displacement. During the testing, the sample was placed in a rubber membrane to minimise flow losses and thus ensure the test setup obeyed the assumption of a closed flow system.

3.2. Experimental setup

Permeability tests were performed for the fractured granite specimen using a high-pressure triaxial apparatus, capable of measuring two-phase flow through rock samples loaded under axial and confining stress (Fig. 2), though for these experiments only single-phase (air) flow was investigated. Axial loading for the tests was achieved through porous stone platens which allowed injection and collection of the flowing fluid. A servo-controlled Instron machine was used to maintain a 1.89 MPa axial load on the specimen for all tests. To investigate the affect of fracture normal confining stress on flow behaviour, a series of tests were carried out at five different confining stress values of 550 kPa, 1000 kPa, 2000 kPa, 3000 kPa and 5000 kPa. Hydraulic oil was used as the cell confining fluid and confining stress was applied using a hydraulic pump. The magnitude of the confining pressure was recorded using a pressure transducer that carries a combined total error band of ±0.75% of the maximum measurement.

Fig. 1. Photo of the fractured granite specimen used for the experimental work.

Once the sample had been taken to the test confining pressure, the test fluid (air) was pumped from the fluid amplification device (an air compressor) to the porous stone platen at the bottom of the sample and collected from an outlet hose connected to the porous stone platen at the top of the sample. Airflow rates through the outlet hose were measured by a film flow meter to a reported accuracy of ±0.5%. Back flow of liquid from the sample was prevented with the use of a check valve at the inlet flow supply. The magnitudes of inflow and outflow fluid pressures were recorded by two independent pressure transducers. The reported combined total error band for the pressure transducers was ±0.75% of the maximum measurement. Various experiments at differing air injection pressures were performed for each confining pressure to produce five independent datasets — i.e. 550 kPa, 1000 kPa, 2000 kPa, 3000 kPa and 5000 kPa confining pressure datasets. Total errors on the various experimental measurements were estimated at ±1.0%.

4. Results and discussion

Table 1 summarises the results of the experimental work for the 550 kPa, 1000 kPa, 2000 kPa, 3000 kPa and 5000 kPa confining pressure experiments, in the form of outlet flow rate measurements corresponding to various inlet and outlet gas pressure combinations. Fig. 3 illustrates the manner by which measured outlet flow rates from the various experiments varied with mean pressure, as calculated from the inlet and outlet pressures in accord with Eq. (4).

From Fig. 3, it can be seen that the measured outlet flow rate is approximately linearly proportional to mean pressure for all measurements made on the 550 kPa, 1000 kPa and 2000 kPa confining pressure experiments and all but the measurement made at the highest mean pressure for the 3000 kPa confining pressure experiment. In the case of the 5000 kPa confining pressure experiment, the four lowest mean pressure measurements obey approximate linearity between mean pressure and outlet flow rate. The linearity of the measured outlet flow v. mean pressure plots is consistent with a Darcian gas flow regime within the fracture, for the majority of the experimental data. Thus, we have assumed that each of the experimental flow cases obeyed Darcian linearity to an extent where the cubic law (9) can be used to estimate

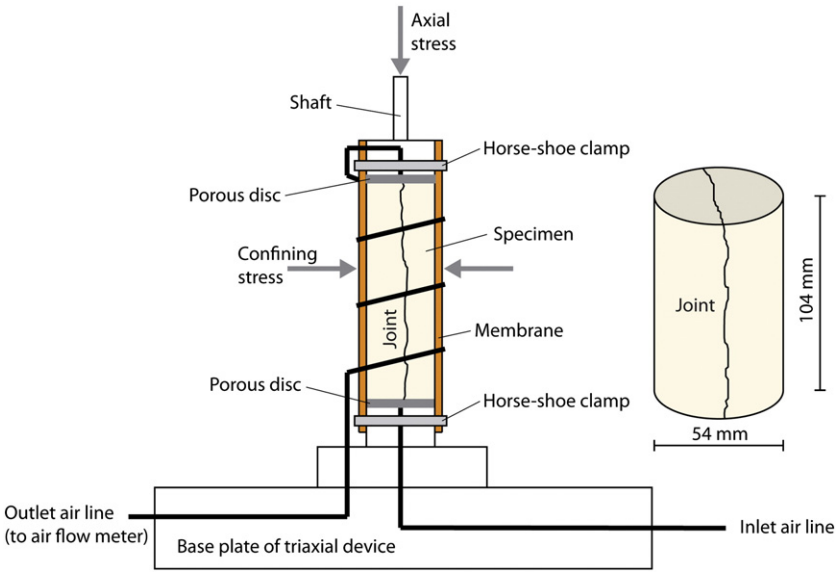

Fig. 2. Experimental setup (after Ranjith et al., 2006, p. 219).

Table 1
Summary table of experimental measurements and calculated flow values.

Cell pressure (kPa)	Air inlet pressure (kPa)	Air Outlet pressure (kPa)	Measured flow rate (mL/min)	Calculated hydraulic aperture (μm)	Calculated superficial flow velocity (m/s)	Calculated permeability $\times 10^{11}$ (m^2)	Calculated Reynolds number	Calculated Forcheimer number
550	125	100	5.1	2.688	0.106	3.898	0.10	0.013
550	150	100	15	2.951	0.285	4.699	0.31	0.034
550	200	100	46	3.202	0.806	5.533	0.95	0.097
550	250	100	79	3.182	1.393	5.464	1.63	0.168
550	300	100	102	3.011	1.901	4.893	2.10	0.230
550	350	100	131	2.922	2.516	4.606	2.70	0.304
550	400	100	159	2.832	3.151	4.326	3.27	0.381
550	450	100	191	2.770	3.870	4.139	3.93	0.468
1000	300	100	44	1.864	0.728	3.409	0.91	0.104
1000	400	100	68	1.748	1.201	2.997	1.40	0.171
1000	500	100	99	1.694	1.804	2.814	2.04	0.256
1000	600	100	132	1.644	2.478	2.651	2.72	0.352
1000	700	100	166	1.597	3.208	2.502	3.42	0.456
1000	800	100	192	1.531	3.870	2.300	3.95	0.550
2000	300	100	34	1.358	0.386	3.617	0.70	0.199
2000	400	100	51	1.260	0.624	3.117	1.05	0.322
2000	500	100	69	1.192	0.893	2.787	1.42	0.461
2000	600	100	92	1.157	1.227	2.626	1.89	0.633
2000	700	100	113	1.115	1.564	2.440	2.33	0.807
2000	800	100	128	1.062	1.861	2.211	2.63	0.960
2000	900	100	142	1.015	2.159	2.021	2.92	1.114
2000	1000	100	157	0.978	2.479	1.875	3.23	1.279
3000	300	100	29	1.125	0.265	3.724	0.60	0.113
3000	400	100	45	1.056	0.438	3.283	0.93	0.187
3000	500	100	65	1.021	0.655	3.066	1.34	0.280
3000	600	100	88	0.996	0.909	2.918	1.81	0.389
3000	700	100	105	0.951	1.136	2.659	2.16	0.486
3000	800	100	123	0.915	1.383	2.465	2.53	0.591
3000	900	100	138	0.878	1.617	2.270	2.84	0.691
3000	1000	100	153	0.847	1.859	2.109	3.15	0.795
3000	1100	100	178	0.835	2.193	2.052	3.66	0.937
3000	1600	100	202	0.678	3.067	1.351	4.16	4.592
5000	600	100	67	0.767	0.539	2.885	1.38	0.363
5000	800	100	103	0.728	0.874	2.597	2.12	0.589
5000	1000	100	128	0.673	1.174	2.221	2.63	0.791
5000	1200	100	157	0.637	1.521	1.991	3.23	1.025
5000	1400	100	169	0.589	1.772	1.701	3.48	2.320
5000	1600	100	179	0.549	2.013	1.478	3.68	2.636
5000	1800	100	194	0.521	2.298	1.332	3.99	3.009
5000	2000	100	206	0.495	2.566	1.204	4.24	3.360
5000	2200	100	234	0.485	2.978	1.154	4.81	3.899

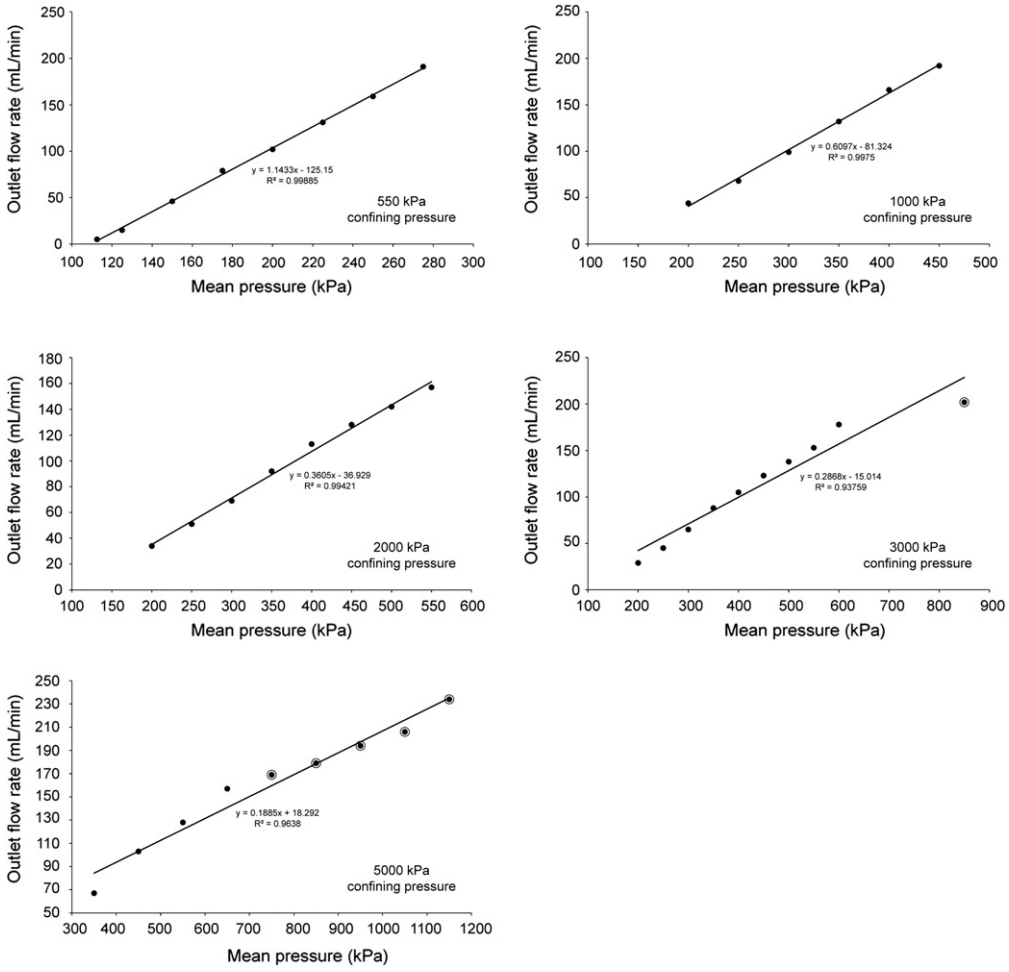

Fig. 3. Measured outlet flow rate v. mean pressure for all experiments with a linear fit to the data. Results for confining pressures of 550 kPa, 1000 kPa, 2000 kPa, 3000 kPa and 5000 kPa each plotted separately. Data that deviate from an approximately linear relationship between outlet flow and mean pressure are circled.

aperture thickness, assuming a gas (air) density of 1.20 kg/m^3 at room temperature (20 °C) and atmospheric pressure (100 kPa) and an air viscosity of 1.8×10^{-5} Pa s at room temperature. Flow area for the fracture was calculated from the hydraulic aperture (determined by the cubic law) multiplied by the sample diameter. The superficial flow velocity was then estimated by dividing measured values for outlet flow rate by calculated values for flow area. The calculated superficial flow velocity was substituted into Eq. (3) to determine a 'representative Darcian permeability' for each experimental measurement. Calculated values for hydraulic aperture, superficial flow velocity and representative Darcian permeability are summarised in Table 1.

Fig. 4 shows that the 'representative Darcian permeability' is dependent on the reciprocal mean pressure of flow (i.e. the inverse of the mean pressure of flow calculated from Eq. (4)). This dependency may be related to inertial effects or to the influence of gas slippage (see Adzumi, 1937; Klinkenberg, 1941). In the case of the gas slippage effect, the theoretical dependence between gas permeability and reciprocal mean pressure is linear and positive (Klinkenberg, 1941). The slopes of the curves of Fig. 4 vary with the reciprocal mean pressure. Thus, it is likely that permeability dependence on mean pressure (Fig. 4) is related to inertial effects on the fracture flow and not gas slippage.

The pressure drop (calculated from the inlet and outlet flow pressure data, the confining pressure and sample length) can be plotted against the calculated superficial velocities for the various experiments to give a graphical representation of Darcy's Law, in accordance with Eq. (3). Such plots for all data from the various confining pressure experiments are given in Fig. 5.

Fig. 5 demonstrates that the data expressed on these Darcian plots are better approximated using a quadratic fit – in the form of the Forchheimer Eq. (14) – than using a linear fit. This is particularly the case for the data from the 3000 kPa and 5000 kPa confining pressure experiments, which showed deviation from linearity for high mean pressures in the measured outlet flow rate v. mean pressure plots of Fig. 3. The results for the 3000 kPa and 5000 kPa confining pressure experiments are replotted for only those test data that obeyed approximate linearity (see non-circled data points of Fig. 3) in Fig. 6.

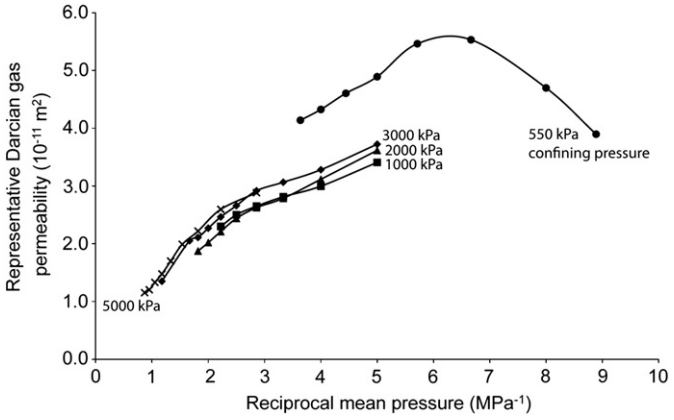

Fig. 4. Calculated representative Darcian gas permeability v. reciprocal mean pressure for experiments carried out at confining pressures of 550 kPa, 1000 kPa, 2000 kPa, 3000 kPa and 5000 kPa.

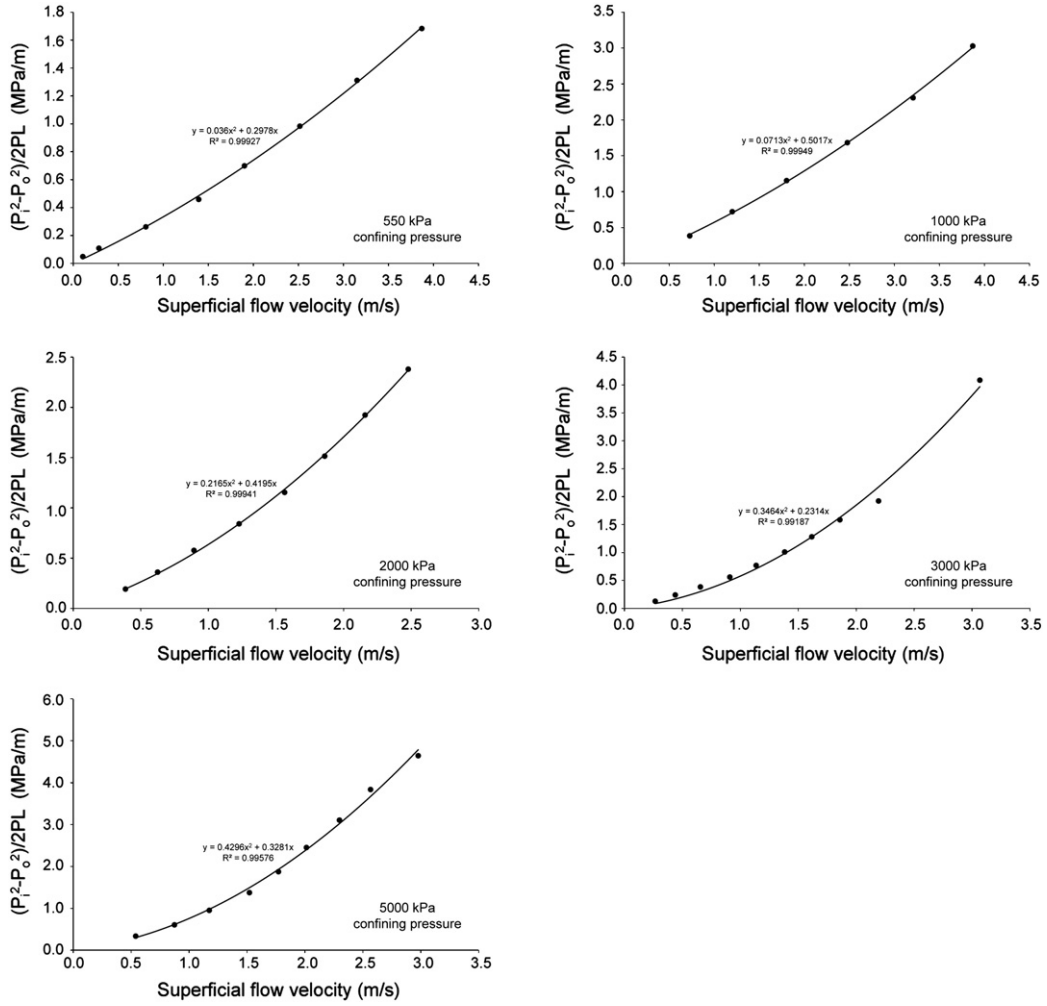

Fig. 5. Pressure drop v. calculated superficial flow velocity plots for all experiments. Results for confining pressures of 550 kPa, 1000 kPa, 2000 kPa, 3000 kPa and 5000 kPa each plotted separately. Trendlines show quadratic fit to the experimental data.

Though the curvature in the reduced dataset of Fig. 6 is not so pronounced as for their equivalents of Fig. 5, the data still shows a form which would be better approximated by a quadratic fit than a linear fit.

The quadratic fits for the flow cases of Figs. 5 and 6 suggest that the Forcheimer number for these flow cases (Eq. (15)) is greater than zero and flow must incorporate a non-linear component — i.e. permeability is dependent on flow velocity and contravenes Darcy's Law. The cubic law (9) that was used above for analysis of the flow data is appropriate only for Darcian flow (Witherspoon et al., 1980). The applicability of the cubic law in the analyses presented here must thus be reviewed.

Approximations to the Darcian (k_1) and non-Darcian (k_2) permeabilities of Eq. (14) can be found (using values for air density and viscosity as above) from the linear and quadratic coefficients, respectively, of the quadratic fits from Figs. 5 and 6. Table 2 summarises the coefficients from the quadratic fits to the experimental data (see Figs. 5 and 6) and shows Darcian and non-Darcian permeabilities calculated from these.

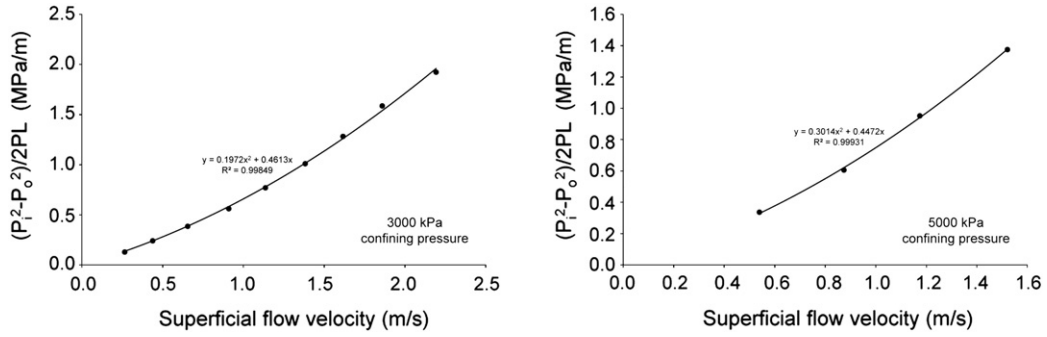

Fig. 6. Pressure drop v. calculated superficial flow velocity plots for confining pressures of 3000 kPa and 5000 kPa. Plots only consider those data of Fig. 3 that obeyed approximate linearity (i.e. the non-circled data of Fig. 3). Trendlines show quadratic fit to the experimental data.

Table 2
Summary of coefficients for quadratic fits shown in Figs. 5 and 6 and Darcian and non-Darcian permeabilities calculated from these. Table entries shaded in grey considered non-linear data points from Fig. 3.

Confining pressure (kPa)	Data included	Linear coefficient	Darcian permeability $\times 10^{11}$ (m^2)	Quadratic coefficient	Gas density (kg/m^3)	Non-darcian permeability $\times 10^4$ (m)
550 kPa	All	0.2978	6.044	0.0360	6.6	1.833
1000 kPa	All	0.5017	3.588	0.0713	12	1.683
2000 kPa	All	0.4195	4.291	0.2165	24	1.109
3000 kPa	All	0.2314	7.779	0.3464	36	1.039
3000 kPa	Linear data, Fig. 3	0.4613	3.902	0.1972	36	1.826
5000 kPa	All	0.3281	5.486	0.4296	60	1.397
5000 kPa	Linear data, Fig. 3	0.4472	4.025	0.3014	60	1.991

If only the data that obeyed approximate linearity in Fig. 3 are considered (i.e. shaded rows of Table 2 were not considered) the non-Darcian permeabilities are relatively constant for the various confining stress experiments. The Darcian permeability for the 550 kPa confining pressure case shows the greatest permeability and the Darcian permeabilities become relatively uniform for the higher confining stress tests – reflecting a permeability decrease of diminishing magnitude with increasing confinement (see Brace et al., 1968) – as one might expect. Thus, the Darcian and non-Darcian permeabilities of Table 2 show good agreement for the various experiments (at differing confining pressure), where only the data that obeyed approximate linearity in Fig. 3 are considered. This result supports a case for the applicability of the cubic law for use as a method for initial determination of superficial flow velocities (from the hydraulic aperture and resultant flow area) in non-linear flow cases. However, Table 2 shows that when the data that departed from approximate linearity in Fig. 3 are considered (i.e. the shaded rows of Table 2), agreement between the calculated Darcian and non-Darcian permeabilities from the various experiments (at differing confining pressure) becomes more tenuous. Thus, it can be seen that the cubic law (9) provides a less satisfactory expression to determine superficial flow velocities as the non-linearity of flow increases.

Reynolds numbers for each test, calculated from the measured flow rate and test specimen dimensions, in accord with Eq. (11), are given in Table 1. Re for the approximately linear flow cases of Fig. 3 vary between $Re<4$ for the lowest confining pressure experiments and $Re\leq 3.5$ for the higher confining pressure experiments. Fracture flow with $Re\geq 1$ displays some degree of non-linearity (Bear, 1972; Zimmerman et al., 2004). However, the cubic law appears to remain applicable for initial analysis of fracture flow in non-Darcian flows where $Re\leq 3.5$ or even $Re<4$, depending on the confining pressure for the fracture flow. The Re for the transition between fields where the cubic law is valid and where it is not valid for the analysis of flow data is dependent on flow pressure and thus will not be independent of the test conditions. Ruth and Ma (1992) and Garrouch and Ali (2001) have suggested that, due to microscopic effects relating to interaction between the solid and flowing fluid in non-Darcian porous flow scenarios, *Fo* may provide a better indication of the degree of influence of inertial effects on flow than Re. *Fo* number can be calculated from the ratio of the quadratic coefficient to the linear coefficient, for the quadratic fits of Figs. 5 and 6, multiplied by the superficial velocity (15). Table 2 shows that for all the cases where the cubic law was applicable, $Fo<1.30$. We recommend that results obtained from the analysis of fracture flow by the cubic law be treated with suspicion where the results of the analysis indicate that $Fo>1.30$.

5. Conclusions

The influence of inertial effects on the flow of fluids through fractured media is a topic of interest for a number of industries, including numerous applications within the energy sector (e.g. production from gas and oil reservoirs, heat extraction from enhanced geothermal systems, coal-bed methane production). The cubic law relates the hydraulic aperture of a fracture to its permeability, for a given fluid experiencing Darcian flow. The extent of the applicability of the cubic law to flow scenarios that incorporate non-Darcian flow is not fully understood.

Flow rate data collected from experiments carried out on air flow through a fractured granite specimen, loaded under triaxial conditions, were reported. Analysis of the flow rate data to obtain flow velocities was carried out using the cubic law, and the coherence of the results obtained was reviewed. Analysis showed that, for flow conditions with moderate non-Darcian behaviour (i.e. flow with 'weak' inertial effects) the cubic law could be successfully applied to obtain meaningful results. The applicability of the cubic law to the non-Darcian flow case was limited to scenarios for which $Re\leq 3.5$ to $Re<4$, depending on flow pressure. *Fo*, determined assuming that the cubic law was valid for the flow system, provides a measure for the applicability of the cubic law that is more robust than the Re (i.e. is relatively independent of flow conditions). The results of our work show that application of the cubic law for calculation of flow velocity from flow rate data is valid for flow cases that, following analysis using the cubic law, return $Fo<1.30$.

References

Adzumi, H., 1937. On the flow of gases through a porous wall. Bull. Chem. Soc. Jpn. 12, 304–312.
Bear, J., 1972. Dynamics of Fluids in Porous Media. American Elsevier, New York.
Brace, W.F., Walsh, J.B., Frangos, W.T., 1968. Permeability of granite under high pressure. J. Geophys. Res. 73, 2225–2236.
Darcy, H., 1856. Les Fountaines Publiques de la Ville de Dijon. Victor Dalmont, Paris.
Forchheimer, P., 1901. Wasserbewegung durch Boden. Z. Ver. Dtsch. Ing. 45, 1782–1788.
Fox, R.W., McDonald, A.T., Pritchard, P.J., 2004. Introduction to Fluid Mechanics. Wiley, New York.
Garrouch, A.A., Ali, L., 2001. Predicting the onset of inertial effects in sandstone rocks. Transp. Porous Media 44, 487–505.
Hassanizadeh, S.M., Gray, W.G., 1987. High velocity flow in porous media. Transp. Porous Media 2, 521–531.
Holditch, S.A., Morse, R.A., 1976. The effects of non-Darcy flow on the behaviour of hydraulically fractured gas wells. J. Pet. Technol. 28, 1169–1179.
Innocentini, M.D.M., Pardo, A.R.F., Salvini, V.R., Pandolfelli, V.C., 1999a. How accurate is Darcy's law for refractories? Am. Ceram. Soc. Bull. 78, 64–68.
Innocentini, M.D.M., Salvini, V.R., Pandolfelli, V.C., Coury, J.R., 1999b. Assessment of Forchheimer's equation to predict the permeability of ceramic foams. J. Am. Ceram. Soc. 82, 1945–1948.
Klinkenberg, L.J., 1941. The permeability of porous media to liquids and gases. Drilling and Production Practice. American Petroleum Institute, New York, pp. 200–213.
Kohl, T., Evans, K.F., Hopkirk, R.J., Jung, R., Rybach, L., 1997. Observation and simulation of non-Darcian flow transients in fractured rock. Water Resour. Res. 33, 407–418.
Mazaheri, A.R., Zerai, B., Ahmadi, G., Kadambi, J.R., Saylor, B.Z., Oliver, M., Brohmal, G.S., Smith, D.H., 2005. Computer simulation of flow through a lattice flow-cell model. Adv. Water Resour. 28, 1267–1279.
Nazridoust, K., Ahmadi, G., Smith, D.H., 2006. A new friction factor correlation for laminar single-phase flows through rock fractures. J. Hydrol. 329, 315–328.
Ranjith, P.G., Choi, S.K., Fourar, M., 2006. Characterization of two-phase flow in a single rock joint. Int. J. Rock Mech. Min. Sci. 43, 216–223.
Reynolds, O., 1883. An experimental investigation of the circumstances which determine whether the motion of water shall be direct or sinuous, and of the law of resistance in parallel channels. Philos. Trans. R. Soc. Lond. 174, 935–982.
Rose, H.E., 1945. On the resistance coefficient–Reynolds number relationship for fluid flow through a bed of granular material. Proc. Inst. Mech. Eng. 153, 154–168.
Ruth, D., Ma, H., 1992. On the derivation of the Forchheimer equation by means of the averaging theorem. Transp. Porous Media 7, 255–264.
Tek, M.R., Coates, K.H., Katz, D.L., 1962. The effect of turbulence on flow of natural gas through porous reservoirs. J. Pet. Technol. 14, 799–806.
Whitaker, S., 1996. The Forchheimer equation: a theoretical development. Transp. Porous Media 25, 27–61.
Witherspoon, P.A., Wang, J.S.Y., Iwai, K., Gale, J.E., 1980. Validity of cubic law for fluid flow in a deformable rock fracture. Water Resour. Res. 16, 1016–1024.
Zimmerman, R.W., Bodvarsson, G.S., 1996. Hydraulic conductivity of rock fractures. Transp. Porous Media 23, 1–30.
Zimmerman, R.W., Al-Yaarubi, A., Grattoni, C.A., 2004. Non-linear regimes of fluid flow in rock fractures. Int. J. Rock Mech. Min. Sci. 41, 384.